Special Issue of the 7th International Advances in Applied Physics and Materials Science (APMAS 2017)

New Aspects of Microwave Absorption in Ferromagnetic Ni-Mn-Sn Thin Films

A. Srinivasan[a,b,*], R. Modak[b], C. Swapna[a] and V.V. Srinivasu[a]
[a]Department of Physics, University of South Africa, Johannesburg 1710, South Africa
[b]Department of Physics, Indian Institute of Technology Guwahati, Guwahati 781039, India

Heusler alloy films sputtered on Si (100) substrates from a Ni-Mn-Sn target under identical conditions but vacuum annealed at slightly different ramping rates at 550 °C (designated as F1 and F2) have nearly equal compositions. Room temperature X-ray diffraction patterns confirmed single phase cubic austenite ($L2_1$) structure in both films. The average grain size of the films varied from 14.4 nm (F1) to 11.9 nm (F2) due to the difference in annealing conditions. Microwave absorption spectra of F1 and F2 recorded at 9.44 GHz showed a non-resonant low field signal and a ferromagnetic resonance signal. Angular variation of ferromagnetic resonance signal analyzed using Landau-Lifshitz-Gilbert equation yielded slightly different effective perpendicular magnetic anisotropy but the same Gilbert damping constant for both films. A comparative study of ferromagnetic resonance linewidth of F1 and F2 reveals the sensitivity of the technique to subtle microstructural variations in the films.

DOI: 10.12693/APhysPolA.134.178

PACS/topics: Heusler alloy, thin film, magnetic anisotropy, ferromagnetic resonance, Gilbert damping

1. Introduction

Novel physical properties such as giant magneto-caloric effect, giant magneto-resistance, large magnetic shape memory effect and martensitic distortion displayed by Ni_2MnZ (Z = Sn, In, Ga, Sb) Heusler alloys have induced tremendous interest among researchers [1–3]. Recent studies portray Ni_2MnZ as futuristic actuator material [4, 5] and environment friendly magnetic refrigerant [6, 7]. However, most of these studies are confined to the bulk form of these alloys.

It is only in the last decade that efforts have been made to develop Ni_2MnZ thin films for possible use in high frequency devices like high-density magnetic recording, magnetic switching, micro inductors, micro transformers, etc. [8, 9]. In general, these thin films exhibit properties which are quite different from their bulk counterparts. This is mainly due to the strong influence of geometry, microstructure and substrate interface on the physical properties of these thin films [10]. Moreover, crystal structure, composition, and sample-preparation conditions of these alloys influence their magnetic properties [11, 12].

Ferromagnetic resonance (FMR) is one of the most popular techniques for evaluating the magnetic quality of ferromagnetic films. FMR provides information about the magnetic moment, magnetic anisotropy, film interface and surface quality, crystalline defects, and magnetic homogeneity of a ferromagnetic film [13, 14].

In this work, resonant microwave absorption of two Ni-Mn-Sn films prepared under identical conditions has been analyzed to understand the sensitivity of this technique to small experimental deviations in sample preparation and processing and their influence on the microstructure of the films. This work is motivated by the fact that such comparative studies have not been reported for these films before.

2. Materials and equipment

Ni-Mn-Sn films were deposited on Si (100) substrate by dc magnetron sputtering from a $Ni_{50}Mn_{37}Sn_{13}$ alloy target. Argon gas pressure of 0.6 Pa and input power of 10 W were used. Prior to deposition, the sputtering chamber was evacuated to $< 10^{-4}$ Pa.

Two sets of films of same thickness were deposited by keeping all deposition conditions identical. As-deposited films were annealed ex situ at 550 °C under residual argon gas pressure of 10^{-3} Pa for 1 h at slightly different ramping rates. The film with lower heating rate was designated as F1 and the other one as F2.

The film thickness measured using a surface profiler (Veeco Dektak 150) was 500 ± 5 nm for both films. Room temperature crystal structure of the films was determined using an X-ray diffractometer (Rigaku TTRAX III) with Cu K_α radiation in grazing-incidence mode. Surface morphology of the films was imaged at room temperature using an atomic force microscope (AFM, Bruker, Innova series). Composition of the annealed films F1 and F2, evaluated using an energy dispersive X-ray spectroscopy unit (EDX, Oxford) attached to a field emission scanning electron microscope, was found to be $Ni_{58.1}Mn_{34.4}Sn_{7.5}$ and $Ni_{57.9}Mn_{35.0}Sn_{7.1}$, respectively.

Magneto-static properties of the films were measured with a vibrating sample magnetometer (VSM, Lakeshore 7410). Microwave absorption spectra were recorded at room temperature using an electron spin resonance (ESR) spectrometer (Bruker EMX EPR) operating at 9.44 GHz with 3 G modulation field. Samples of

*corresponding author; e-mail: asrini@iitg.ernet.in

size $\sim 2 \times 2$ mm^2 tethered to the flat tail of a fused silica rod, could be positioned with angular accuracy of $\pm 1°$.

3. Results and discussion

X-ray diffraction (XRD) patterns of F1 and F2 films revealed the presence of (111) and (200) super-lattice peaks and the absence of any prominent impurity peak, confirming the single phase austenite structure with $L2_1$ ordering (space group: $Fm\bar{3}m$). The lattice constant of films F1 and F2 deduced by Rietveld refinement method using "FullProf" software is 5.99 Å and 5.97 Å, respectively. The average crystallite (grain) size was estimated to be 14.4 ± 0.2 nm (F1) and 11.9 ± 0.2 nm (F2) from profile analysis of the most intense (220) reflection. The slightly higher ramping rate used during annealing resulted in a slightly contracted unit cell and smaller average grain size in F2 film.

Average roughness R_a and root mean square roughness $R_{r.m.s}$ of the films were estimated from AFM images using "Gwyddion" software to be 1.0 and 0.6 nm for F1 and 1.3 and 0.9 nm for F2. F2 has higher surface roughness as compared to F1 due to the faster heating rate.

M–H loops were recorded at room temperature with the magnetic field along film plane (in-plane) and normal to the film plane (out of plane) orientations (not shown here). In-plane loops exhibit very high retentivity and soft magnetic nature, whereas the out-of-plane loops show very low retentivity. Easy axis of magnetization of both the films was along the film plane. In-plane M–H loops of F1 and F2 show that F1 has slightly higher moment ($M_s = 270$ emu/cc) when compared to F2 ($M_s = 255$ emu/cc). This is due to the slightly higher average crystallite size for F1, as it is well known that the magnetization of Heusler alloys is strongly dependent on crystalline quality [11].

Figures 1a and b show the superposed microwave absorption spectra of forward (−500 Oe to +9000 Oe) and reverse (+9000 Oe to −500 Oe) sweeps of the magnetic fields with in-plane ($\theta_H = 90°$) orientation. Both F1 and F2 exhibit two absorption signals, one at low field and another at higher field. The higher field signal is resonant in nature as it exhibits no hysteresis, i.e., the resonance field H_r (value of the field at which the derivate curve crosses the magnetic field axis) does not shift during the forward and reverse sweeps. It can be identified as the FMR signal. Since this work is primarily focused on the magneto-static and magneto-dynamic property comparison of the two films, further analysis will be confined to the resonant FMR signal.

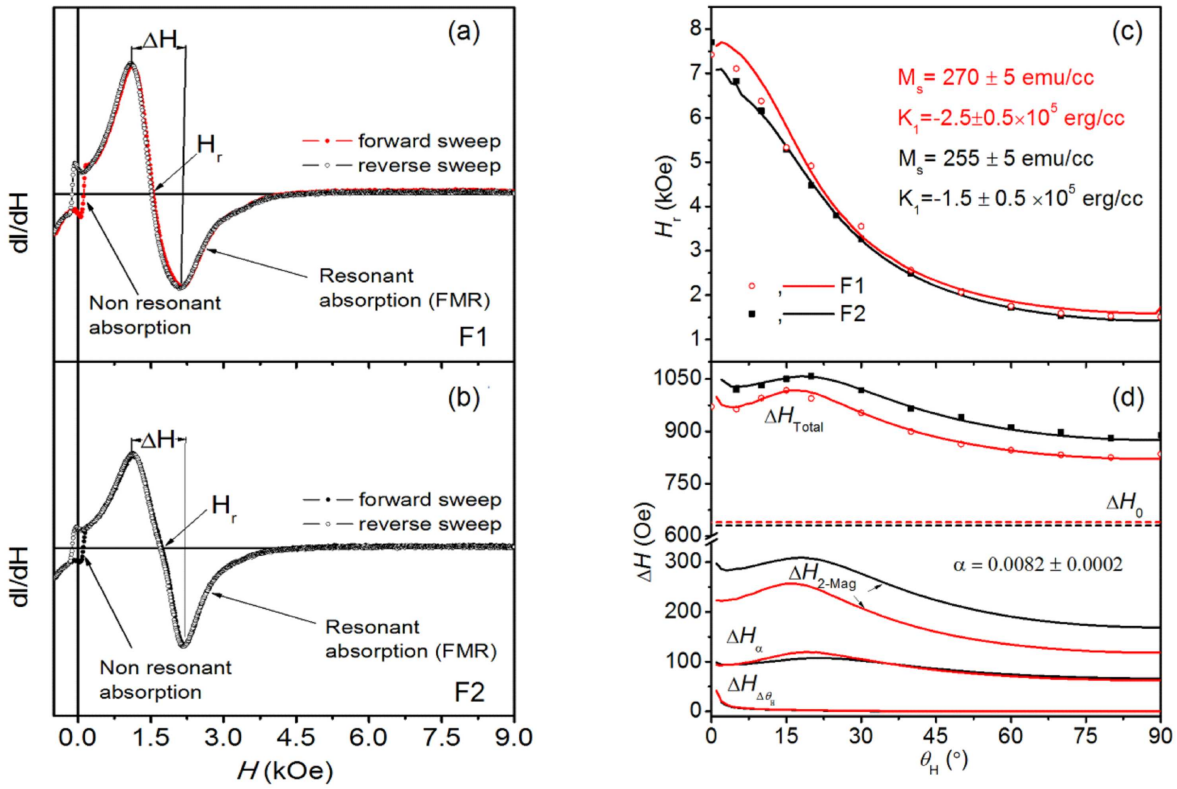

Fig. 1. Microwave absorption spectra dI/dH of the films recorded in forward (−500 Oe to +9000 Oe) and reverse (+9000 Oe to −500 Oe) sweeps of the magnetic fields H for in plane orientation (90°) of the films (a) F1 and (b) F2. (c) Variation of FMR resonance field H_r with θ_H for F1 and F2 films. Symbols represent experimental data and solid lines correspond to the fit to Eq. (4). (d) Angular dependence of linewidth ΔH along with the individual contributions $\Delta H_{2\text{-mag}}$, ΔH_α and $\Delta H_{\Delta\theta}$.

Room temperature FMR spectra recorded for different magnetization M precessional frequencies f and polar angles θ_H at 9.44 GHz can be analyzed numerically to evaluate the magneto-dynamic properties and Gilbert damping constant. We begin the analysis by considering the phenomenological equation of spin dynamics described by the Landau-Lifhitz-Gilbert equation of motion [15, 16],

$$\frac{\partial \boldsymbol{M}}{\partial t} = -\gamma\left(\boldsymbol{M}\times\boldsymbol{H}_{\text{eff}}\right) + \frac{G}{\gamma M_{\text{s}}^2}\left[\boldsymbol{M}\times\frac{\partial \boldsymbol{M}}{\partial t}\right]. \qquad (1)$$

Here H_{eff} is the effective magnetic field acting on M, $\gamma = g\mu_B/\hbar$, $G = \gamma\alpha M_{\text{s}}$ is related to the intrinsic relaxation rate of the material, and α is the Gilbert damping constant. The total magnetic free-energy density of a ferromagnetic thin film is [17, 18],

$$E = -M_{\text{s}}H\left[\sin\theta_H\sin\theta_M\cos\left(\varphi_M-\varphi_H\right)+\cos\theta_H\cos\theta_M\right]$$
$$+2\pi M_{\text{s}}^2\cos^2\theta_M - K_1\cos^2\theta_M. \qquad (2)$$

The first three terms correspond to the Zeeman, dipolar demagnetization energy and perpendicular anisotropy energy, respectively. Here, $\varphi_H(\varphi_M)$ is in-plane angle between $H(M)$ and x-axis, and $\theta_H(\theta_M)$ is the polar angle between $H(M)$ and z-axis. M_{s} is the saturation magnetization and K_1 represents other first-order (intrinsic) anisotropy energy contributions, except the shape anisotropy. The resonance frequency f_{r} of the uniform precession mode is deduced from the energy density by using the following expression [19],

$$f_{\text{r}}^2 = \left(\frac{\gamma}{2\pi}\right)^2\frac{1}{M_{\text{s}}^2\sin^2\theta_M}\left[\frac{\partial^2 E}{\partial\theta_M^2}\frac{\partial^2 E}{\partial\varphi_M^2}-\left(\frac{\partial^2 E}{\partial\theta_M\partial\varphi_M}\right)^2\right]. \qquad (3)$$

The derivatives are evaluated at equilibrium positions of M and H. The solution for the resonance frequency for this configuration can be expressed by the equation,

$$f_{\text{r}} = \frac{\gamma}{2\pi}\left[\left(H\cos\left(\theta_M-\theta_H\right)-4\pi M_{\text{eff}}\cos 2\theta_M\right)\right.$$
$$\left.\times\left(H\cos\left(\theta_M-\theta_H\right)-4\pi M_{\text{eff}}\cos^2\theta_M\right)\right]^{0.5}. \qquad (4)$$

The magnetic relaxation analysis of our thin film has been carried out from θ_H dependence of FMR linewidth. Various sources of damping contribute to the total peak to peak linewidth ΔH such as,

$$\Delta H = \Delta H_0 + \Delta H_\alpha + \Delta H_{\text{2-mag}} + \Delta H_{\Delta\theta_H}, \qquad (5)$$

where ΔH_0 is the residual linewidth which depends on the film quality, ΔH_α is due to Gilbert damping, $\Delta H_{\text{2-mag}}$ comes from 2-magnon scattering, and $\Delta H_{\Delta\theta_H}$ is related to the inhomogeneous broadening. Our previous work [18] provides detailed expressions for all linewidth broadening terms and the same may be referred to if desired.

Numerical fitting of Eq. (4) to the experimental data recorded from in-plane orientation (90°) to out-of-plane (0°) of the film with respect to the applied magnetic field (cf. Fig. 1c) yields an estimate of the perpendicular effective magnetic anisotropy K_1 of the films. It is observed that with the change in annealing condition, a slight change in K_1 from $-2.5\pm0.5\times10^5$ erg/cc (for F1) to $-1.5\pm0.5\times10^5$ erg/cc (for F2) is noticed.

Magnetic relaxation dynamics of the films was investigated using angular dependence of ΔH at 9.44 GHz. θ_H dependence of ΔH was estimated numerically using Eq. (5) and the corresponding fit to experimental data is shown in Fig. 1d. The independent contributions of magnetic damping from different sources are also shown in Fig. 1d. Gilbert constant of 0.0082 ± 0.0002 estimated for both films at 9.44 GHz is in agreement with previously published results on Ni-Mn-Sn films [18, 20–22].

In the present linewidth analysis, a significant contribution to the total linewidth originates from 2-magnon scattering. A careful look at Fig. 1c,d would reveal that although angular variations of H_{r} for both films are almost similar, a noticeable deviation is found in the linewidth variation, which is related to the spin relaxation process and is very much dependent on the microstructure of the films. Two crucial factors contribute to the observed linewidth: one is the Gilbert damping term ΔH_α which is an internal property of the material and other is 2-magnon scattering term $\Delta H_{\text{2-mag}}$ which depends on various extrinsic parameters related to the material nature. In this analysis, we found the ΔH_α term remains nearly the same for both films, which is in expected lines since both the films have the same crystal structure and nearly the same composition. But the 2-magnon contribution in both films is found to be very different, with F2 exhibiting a higher 2-magnon contribution.

One can relate this distinctive difference in 2-magnon scattering in the two films with the microstructural variations between them. From XRD analysis, we found a smaller grain size for F2, indicating more grain boundaries. This tends to create more scattering centers for the magnons. In addition, the surface roughness of F2 is higher than that of F1 which would also increase the magnon scattering in the former. Thus, higher 2-magnon contribution in F2 can be accounted for by the increased grain boundaries and higher surface roughness as compared to F1.

4. Conclusions

Ni-Mn-Sn films with cubic $L2_1$ phase have been successfully grown on Si(100) substrate by DC magnetron spattering. Deposition from the same target, with slightly modified heating rates during annealing, resulted in some microstructural variations between the films. Angular variation FMR analysis revealed the presence of effective perpendicular magnetic anisotropy $K_1 \approx -2.5\pm0.5\times10^5$ erg/cc for F1 and $-1.5\pm0.5\times10^5$ erg/cc for F2 and Gilbert damping constant $\alpha = 0.0082\pm0.0002$ for both films. FMR linewidth has been found to be sensitive to microstructural variations in the films due to changes of grain boundary and surface roughness. This study shows that FMR can be used as an effective tool to analyze minor microstructural changes influencing the magnetic quality of otherwise similar magnetic thin films.

References

[1] V.V. Khovaylo, T. Kanomata, T. Tanaka, M. Nakashima, Y. Amako, R. Kainuma, R.Y. Umetsu, H. Morito, H. Miki, *Phys. Rev. B* **80**, 144409 (2009).

[2] S. Singh, C. Biswas, *Appl. Phys. Lett.* **98**, 212101 (2011).

[3] R. Kainuma, Y. Imano, W. Ito, Y. Sutou, H. Morito, S. Okamoto, O. Kitakami, K. Oikawa, A. Fujita, T. Kanomata, K. Ishida, *Nature* **439**, 957 (2006).

[4] V.A. Chernenko, E. Cesari, V.V. Kokorin, I.N. Vitenko, *Scr. Metall. Mater.* **33**, 1239 (1995).

[5] K. Ullakko, J.K. Huang, C. Kantner, R.C. O'Handley, V.V. Kokorin, *Appl. Phys. Lett.* **69**, 1966 (1996).

[6] W. Guan, Q.R. Liu, B. Gao, S. Yang, Y. Wang, M.W. Xu, Z.B. Sun, X.P. Song, *J. Appl. Phys.* **109**, 07A903 (2011).

[7] A.P. Kazakov, V.N. Prudnikov, A.B. Granovsky, A.P. Zhukov, J. Gonzalez, I. Dubenko, A.K. Pathak, S. Stadler, N. Ali, *Appl. Phys. Lett.* **98**, 131911 (2011).

[8] Ming Xu, T.M. Liakopoulos, C.H. Ahn, Suk Hee Han, Hi Jung Kim, *IEEE Trans. Magn.* **34**, 1369 (1998).

[9] N. Teichert, A. Boehnke, A. Behler, B. Weise, A. Waske, A. Hütten, *Appl. Phys. Lett.* **106**, 192401 (2015).

[10] A. Ishida, V. Martynov, *MRS Bull.* **27**, 111 (2002).

[11] R. Vishnoi, D. Kaur, *Surf. Coatings Technol.* **204**, 3773 (2010).

[12] R. Vishnoi, D. Kaur, *J. Appl. Phys.* **107**, 103907 (2010).

[13] S.I. Patil, D. Tan, S.E. Lofland, S.M. Bhagat, I. Takeuchi, O. Famodu, J.C. Read, K.-S. Chang, C. Craciunescu, M. Wuttig, *Appl. Phys. Lett.* **81**, 1279 (2002).

[14] V.I. Kozlov, *Russ. Electr. Eng.* **85**, 322 (2014).

[15] L.D. Landau, E.M. Lifshitz, *Phys. Z. Sowiet Union* **8**, 153 (1935).

[16] T.L. Gilbert, *Phys. Rev.* **100**, 1243 (1955).

[17] M.T. Johnson, P.J.H. Bloemen, F.J.A. den Broeder, J.J. De Vries, *Reports Prog. Phys.* **59**, 1409 (1996).

[18] R. Modak, B. Samantaray, P. Mandal, A. Srinivasan, *J. Alloys Compd.* **692**, 529 (2017).

[19] O. Acher, S. Queste, M. Ledieu, K.-U. Barholz, R. Mattheis, *Phys. Rev. B* **68**, 184414 (2003).

[20] J. Dubowik, K. Załęski, H. Głowiński, I. Gościańska, *Phys. Rev. B* **84**, 184438 (2011).

[21] J. Dubowik, A. Ehresmann, G. Kakazei, S.A. Bunyaev, *Acta Phys. Pol. A* **121**, 1121 (2012).

[22] R. Modak, B. Samantaray, P. Mandal, A. Srinivasan, *Appl. Phys. A* **122**, 252 (2016).